

## Wide-field (sub)millimeter continuum surveys of protoclusters: Clues to the origin of the IMF

Frédérique Motte

*California Institute of Technology, Mail Stop 320-47, 1200 E. California  
Blvd., Pasadena, CA 91125, USA*  
*Max-Planck-Institut für Radioastronomie, Auf dem Hügel 69, 53121  
Bonn, Germany*

Philippe André

*CEA, DSM, DAPNIA, Service d'Astrophysique, C.E. Saclay,  
F-91191 Gif-sur-Yvette Cedex, France*

**Abstract.** Recent (sub)millimeter continuum surveys of nearby star-forming regions have revealed a wealth of new, cold cloud fragments. Those which are small-scale (diameter  $\lesssim 10\,000$  AU), starless, and gravitationally bound are good candidates for being the direct progenitors of protostars, i.e., the structures within which individual protostellar collapse is initiated. The mass spectrum of these protocluster condensations is reminiscent of the stellar initial mass function (IMF), suggesting the IMF is partly determined by cloud fragmentation at the pre-stellar stage of star formation.

### 1. Introduction

The question of the origin and possible universality of the initial mass function (IMF), which is crucial for both star formation and galactic evolution, remains a matter of debate (e.g. Elmegreen, this volume). In the past, numerous molecular line studies of cloud structure have attempted, without success, to relate the mass spectrum of observed clumps to the stellar IMF (see, e.g., Williams, Blitz, & McKee 2000 and references therein). The reason of this failure is presumably that most CO clumps are not gravitationally bound and reflect more the characteristics of the low-density outer parts of molecular clouds than the initial conditions of protostellar collapse (e.g. Kramer et al. 1998).

The advent of sensitive bolometer arrays on large (sub)mm radiotelescopes has recently made possible extensive surveys for protostars and their prestellar precursors in nearby star-forming regions (see, e.g., review by André, Ward-Thompson, & Barsony 2000). Wide-field millimeter continuum mapping of molecular clouds was first performed using the (19- and 37-channel) MPIfR bolometer arrays (MAMBO) at the IRAM 30m telescope (e.g. Chini et al. 1997; Motte, André, & Neri 1998 – hereafter MAN98). More recently, the bolometer cameras SCUBA and SHARC have been used at the JCMT and CSO radiotelescopes (e.g. Lis et al. 1998; Johnstone et al. 2000 – hereafter JWM00; Motte

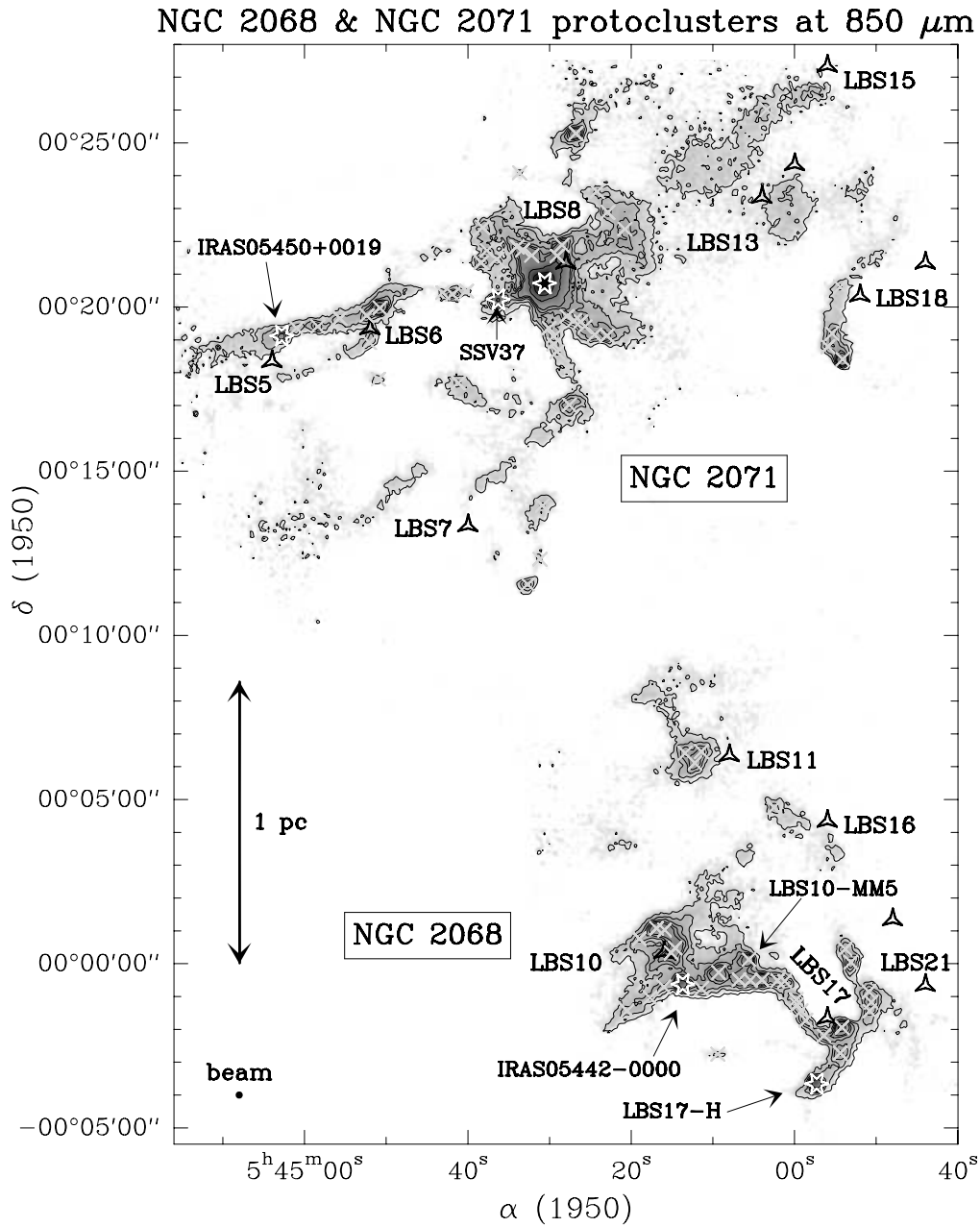


Figure 1. Dust continuum mosaic of the NGC 2068 and NGC 2071 protoclusters at 850  $\mu\text{m}$ , including the CS dense cores LBS5 to LBS8, LBS10, LBS11 and LBS13 to LBS21 (from Lada, Bally, & Stark 1991, marked with triangles). The data were taken with the SCUBA bolometer array at the JCMT. Starless condensations are denoted by crosses and young embedded stars by star markers.

et al. 2001 – hereafter MAWB01, see Fig. 1). At the same time, mosaics of star-forming cloud cores have been obtained with the Owens Valley millimeter array (OVRO), over somewhat smaller areas but with higher angular resolution than single-dish bolometer observations (e.g. Testi & Sargent 1998 – hereafter TS98).

These (sub)mm continuum surveys have detected a large number of starless cloud fragments in the  $\rho$  Oph (MAN98; JWM00), Serpens (TS98), OMC1 (Coppin et al. 2000 – hereafter CGJH00), NGC 1333 (Sandell & Knee 2000 – hereafter SK01), and NGC 2068/2071 (MAWB01) cluster-forming regions. Some of the starless fragments, dubbed here *protocluster condensations*, are likely to be the direct progenitors of protostars (see Sect. 2.2 below). When such condensations are carefully extracted from their surrounding cloud (see Sect. 2.3), the associated mass spectrum is found to resemble the shape of the stellar IMF (Sect. 3.1). This has important implications for the origin of the IMF in clusters (Sect. 4). We here give an overview of these recent submillimeter results and compare the methods employed in the various published studies.

## 2. Analysis of cloud structure

Relating cloud structure to star formation is a difficult task which requires a careful analysis motivated by physical questions such as: What is the size scale of protostellar collapse? How can we select those cloud fragments that are the potential progenitors of protostars? How can we accurately measure the mass reservoirs involved in individual collapse? Possible answers are proposed below.

### 2.1. Estimating the characteristic size scale of protostellar collapse

Numerous CO studies have shown that the overall structure of molecular clouds is fractal and probably shaped by turbulence, in both quiescent and star-forming regions (e.g. Elmegreen & Falgarone 1996; Heithausen et al. 1998). On the other hand, there is a growing body of evidence that this fractal structure breaks down once self-gravity takes over at the high densities and small lengthscales characteristic of individual protostellar collapse.

First, the CO maps of the Taurus cloud cannot be described by a single fractal dimension (Blitz & Williams 1997). Second, the dense cores observed within molecular clouds appear to be “coherent”, i.e., largely devoid of turbulence, in their inner  $0.1 \text{ pc} \simeq 20\,000 \text{ AU}$  parts (Goodman et al. 1998). Third, mid-infrared absorption images of isolated starless dense cores taken with ISOCAM aboard ISO show that these cores are typically finite-sized structures (Bacmann et al. 2000; Bacmann, André, & Ward-Thompson, this volume). Finally, (sub)mm continuum maps of optically thin dust emission also indicate finite sizes for protostellar envelopes. The radial intensity profiles observed for the envelopes of nearby protostars are indeed consistent with a power-law density structure merging into some background cloud emission beyond some outer radius  $R_{\text{out}}$  (MAN98; Motte & André 2001; see also Fig. 2a). The envelope outer radii are measured to be typically  $\sim 5\,000 \text{ AU}$  in  $\rho$  Oph and NGC 2068/2071 while being  $\gtrsim 10\,000 \text{ AU}$  in Taurus. These outer sizes may result from truncation by the local ambient cloud pressure  $P_s$ , varying from  $\langle P_s \rangle \sim 5 - 10 \times 10^5 k_B \text{ cm}^{-3} \text{ K}$

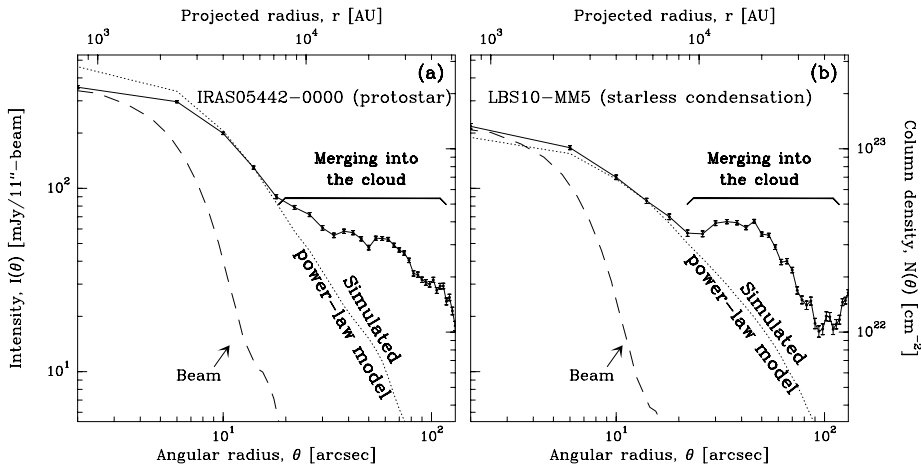


Figure 2. Circularly averaged radial intensity profiles of a protostellar envelope (a) and a starless condensation (b) in the NGC 2068 protocluster, derived from a 1.3 mm continuum map taken with MAMBO at the IRAM 30m telescope. Both profiles are clearly resolved and merge into some background cloud emission at  $R_{\text{out}} \sim 6\,000 - 8\,000$  AU. This behavior is qualitatively similar to that observed in  $\rho$  Oph (see Figs. 4c-d of MAN98), Taurus, and Perseus (see, e.g., Figs. 3f and 4g of Motte & André 2001; André, Motte, & Belloche, this volume).

in dense protoclusters such as  $\rho$  Oph and NGC 2068/2071, to  $\langle P_s \rangle \sim 0.5 \times 10^5 k_B \text{ cm}^{-3} \text{ K}$  in regions of more distributed star formation such as Taurus.

*The typical size observed for (young) protostellar envelopes in a given star-forming region provides a natural lengthscale which is likely to be characteristic of the detached cloud fragments participating in individual protostellar collapse.*

## 2.2. Selecting the possible progenitors of protostars

Guided by the ideas outlined in § 2.1 above, MAN98 and MAWB01 have used a multiresolution wavelet technique (e.g. Starck, Murtagh, & Bijaoui 1998) to analyze their (sub)mm maps of the  $\rho$  Oph and NGC 2068/2071 protoclusters. With this technique, it is possible to separate small-scale fragments from structures larger than the characteristic outer size of protostellar envelopes. Note that the wavelet analysis is not subject to human bias, unlike the “visual inspection method” used by e.g. SK01 in NGC 1333.

As illustrated in Fig. 3 for the  $\rho$  Oph-F region, the procedure consists in decomposing the original image in a number of views of the same field at different spatial scales. For simplicity, only two such views are shown in Fig. 3. The “small-scale” view (bottom right of Fig. 3) has been adjusted so as to trace circumstellar envelopes (or disks) around embedded young stellar objects (YSOs). In addition, the same view reveals several compact starless fragments (e.g. F-MM1 and F-MM2 in Fig. 3). These are not associated with any centimeter radio continuum emission or near-/mid-IR emission (MAN98). They are even often

seen in *absorption* by ISOCAM at  $7\ \mu\text{m}$  against the diffuse mid-IR emission arising from the cloud’s outer layers (e.g. Motte et al. 1998b). These small-scale fragments are good candidates for being pre-stellar condensations (see below). On the other hand, the structures that show up in the “large-scale” view (bottom left of Fig. 3) correspond to dense cores already known from DCO<sup>+</sup>, CS, or NH<sub>3</sub> studies with  $\sim$  arcmin resolution (e.g. Loren, Wootten, & Wilking 1990). In protoclusters, such dense cores are typically the sites of multiple protostellar collapse and correspond to the background environment of several smaller-scale condensations. In regions of isolated star formation (e.g. Taurus), dense cores of similar sizes generally give birth to only one or two stars (cf. Myers 1998).

The  $\rho$  Oph starless condensations identified in this way by MAN98 have relatively narrow linewidths and are close to gravitational virial equilibrium according to recent observations in high-density molecular tracers (see Belloche, André, & Motte, this volume). Furthermore these condensations, as well as those of MAWB01 in NGC 2068/2071 have spheroidal shapes (aspect ratio  $\sim 0.6$ , see also CGJH00). All of this suggests that the condensations have dissipated (most of) their initial magnetic turbulent support and are on the verge of collapse. In  $\rho$  Oph, some of them already show spectroscopic evidence of inward motions (see Belloche et al., this volume). Based on these characteristics and the similarity with protostellar envelopes, we argue that the starless condensations identified in the (sub)mm continuum are likely to be *pre-stellar in nature and the direct progenitors of accreting (i.e. Class 0, Class I) protostars*.

In the Serpens core, the OVRO interferometer study of TS98 filtered out all cloud structures larger than  $\sim 9\,000$  AU in diameter. As this is comparable to the size of protostellar envelopes in Serpens, the sources detected by TS98 are probably “protocluster condensations” in the same sense as above. However, line and centimeter radio continuum observations would be needed to confirm that these condensations are self-gravitating and pre-stellar in character.

In their independent study of the  $\rho$  Oph protocluster, JWM00 analyzed cloud structure without reference to any circumstellar lengthscale. In practice, they nevertheless selected fragments smaller than  $21\,000$  AU in diameter, owing to the Gaussian filter applied to remove reduction artifacts from the SCUBA data. They identified as “clumps” all the structures associated with a local maximum in their map, regardless of size, global shape, or substructure. Some of these clumps are very diffuse and may be transient features confined by external pressure rather than bound by gravity (cf. Bertoldi & McKee 1992). Moreover, several of the JWM00 clumps are and/or will clearly be the sites of multiple protostellar collapse (e.g. the clump associated with IRS43, CRBR85, and F-MM2 in Fig. 3). Thus, in general, the structures selected by JWM00 do not seem to be truly representative of collapse initial conditions and cannot be taken as the direct progenitors of protostars.

### 2.3. Making reliable measurements of the collapse mass reservoir

In order to estimate the total mass available for local gravitational collapse, one first needs to quantify the importance of the background cloud surrounding each pre-stellar condensation. This is definitely the most difficult step in the analyses of MAN98, CGJH00, and MAWB01. CGJH00 assumed that all their condensations were essentially unresolved (i.e. diameter  $\lesssim 6\,000$  AU in their

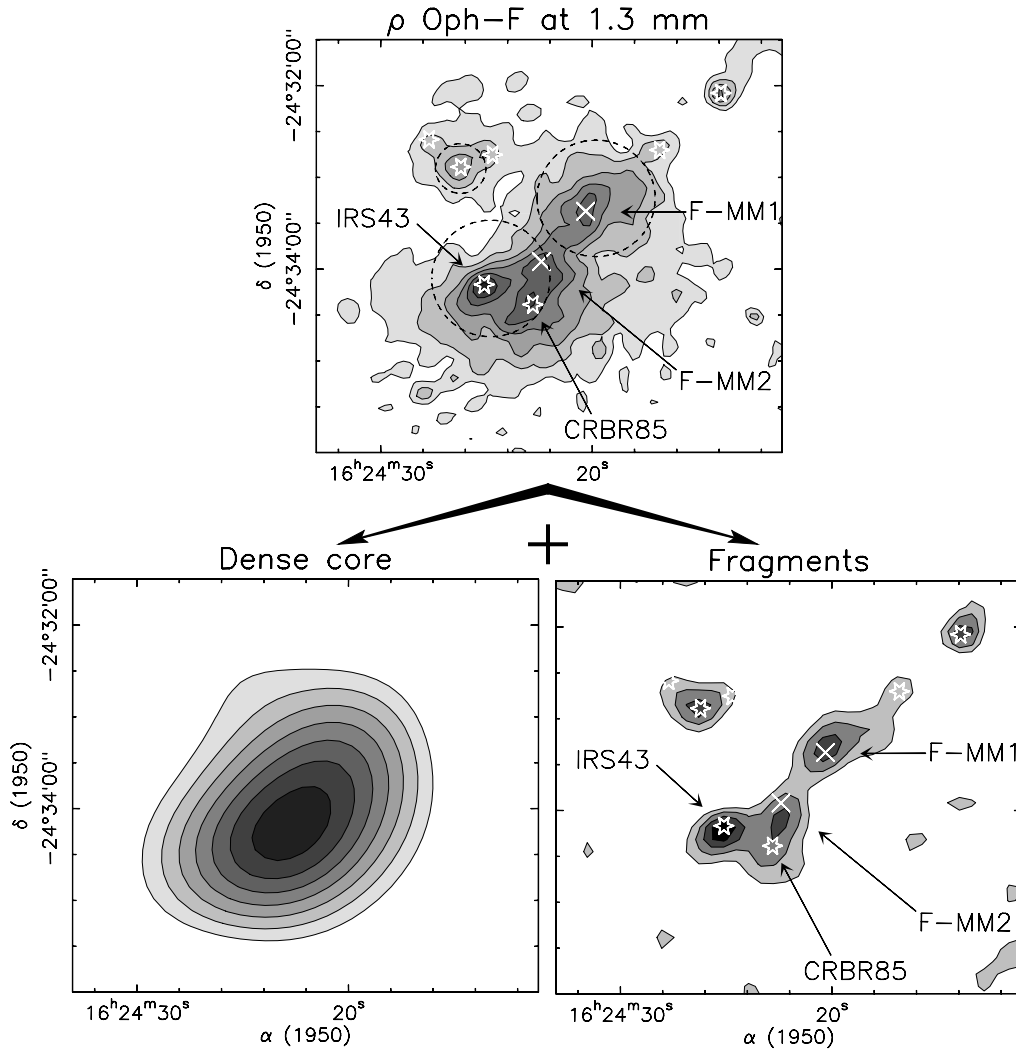


Figure 3. Illustration (in the case of  $\rho$  Oph-F) of the multiresolution wavelet technique used by MAN98 to analyze the structure of the  $\rho$  Oph cloud. The original 1.3 mm continuum map (top) is decomposed into a large-scale view sensitive to structures  $\gtrsim 10\,000$  AU in diameter (bottom left) and a small-scale view tracing small-scale fragments  $\sim 1\,000$ – $6\,000$  AU in diameter (bottom right). The dashed large circles represent the sizes of the clumps identified by JWM00.

case) and thus estimated only lower limits to the corresponding mass reservoirs. The analysis of MAN98 and MAWB01 is more sophisticated as it uses the radial intensity profiles of the condensations to determine their outer radii (e.g. § 2.1 and Fig. 2b). This makes it possible to filter the background very effectively and to get an accurate measurement of the collapse mass reservoir, without any a priori assumption about the fragment shape. It is however a time-consuming process that cannot be easily automated. The condensations must also be spatially resolved which, in practice, limits the technique to nearby regions.

As for TS98, they integrated the emission detected toward the point-like sources identified in their OVRO 3.3 mm mosaic. They did not correct for the physical size of the mass reservoir which may be slightly larger than the 9000 AU diameter of the interferometric filter.

In another approach, JWM00 used a variant of the clump finding algorithm of Williams, de Geus, & Blitz (1994) which assumes that a fragment ends at the last significant contour surrounding it. Such a boundary is signal-to-noise dependent and not necessarily related to the physical outer radius resulting from, e.g., truncation by the pressure of the background cloud.

After source extraction and background subtraction, the masses of the condensations identified are estimated from the measured (sub)mm fluxes assuming dust properties (temperature and opacity) adapted to pre-stellar cores (see e.g. MAN98). At least far from massive YSOs, starless condensations are expected to have low temperatures  $T_{\text{dust}} \lesssim 10 - 15$  K, as they are well shielded from external heating by cosmic rays and the interstellar radiation field (e.g. Masunaga & Inutsuka 2000; Evans et al. 2001).

### 3. Overview of results

With present instruments, wide-field (sub)mm surveys of nearby ( $d < 500$  pc) protoclusters are limited to the detection of  $\gtrsim 0.02 M_{\odot}$  condensations and are only complete down to  $\gtrsim 0.1 M_{\odot}$ . Table 1 lists several of the above-mentioned submm continuum studies, along with the related molecular line survey of Taurus by Onishi et al. (2001, this volume – hereafter OMKF01). The characteristics of the cloud fragments found in each study are given in the last column.

#### 3.1. Mass distribution of protocluster condensations

When one carefully selects the (sub)mm fragments seen on the same spatial scales as protostellar envelopes (cf. § 2.2), the resulting mass spectrum appears to mimic the shape of the stellar IMF (see MAN98; TS98; MAWB01 and Fig. 4). The cumulative mass spectra of the pre-stellar condensations identified in the  $\rho$  Oph, Serpens, and NGC 2068/2071 protoclusters approximately follow the Salpeter power-law (i.e.  $N(> m) \propto m^{-1.35}$ , Salpeter 1955) for  $m > 0.3 - 0.5 M_{\odot}$ ,  $\gtrsim 0.4 M_{\odot}$  and  $\gtrsim 0.8 M_{\odot}$ , respectively. At lower masses, the  $\rho$  Oph mass spectrum flattens to  $N(> m) \propto m^{-0.5}$  as does the stellar IMF (e.g. Kroupa, Tout, & Gilmore 1993). This suggests that *the protocluster condensations detected in the (sub)mm continuum will form individual stars/systems with a high efficiency roughly independent of mass*. More quantitatively, comparison of the pre-stellar mass spectrum of MAN98 with the mass spectrum determined by Bontemps et al. (2001) for pre-main sequence objects suggests that the local star formation

Table 1. Summary of recent studies of cloud fragmentation

Authors & region	Observations	Fragment characteristics <sup>(1)</sup>
MAN98 $\rho$ Oph, 150 pc	At 1.3 mm with MAMBO/IRAM 30m	59, pre-stellar and self-gravitating 1 000 – 6 000 AU, 0.05 – 3 $M_{\odot}$
TS98 Serpens, 310 pc	At 3 mm with OVRO	26, pre-stellar 700 – 9 000 AU, 0.5 – 25 $M_{\odot}$
CGJH00 OMC1, 450 pc	At 850 $\mu$ m with SCUBA/JCMT	39, pre-stellar or protostellar $\lesssim$ 6 000 AU, 0.1 – 100 $M_{\odot}$
JWM00 $\rho$ Oph, 150 pc	At 850 $\mu$ m with SCUBA/JCMT	34, starless and still evolving $\sim$ 1 500 – 10 000 AU, 0.03 – 10 $M_{\odot}$ <sup>(2)</sup>
SK01 NGC 1333, 220 pc	At 850 $\mu$ m with SCUBA/JCMT	33, pre-stellar or protostellar 500 – 8 000 AU, 0.02 – 2.5 $M_{\odot}$ <sup>(2)</sup>
MAWB01 NGC2068/71, 400 pc	At 850 $\mu$ m with SCUBA/JCMT	70, pre-stellar 1 600 – 13 000 AU, 0.3 – 6 $M_{\odot}$
OMKF01 Taurus, 150 pc	H <sup>13</sup> CO <sup>+</sup> (1 – 0) at the NRO 45 m	45, starless < 20 000 AU, 0.4 – 25 $M_{\odot}$

<sup>(1)</sup> Number, pre-stellar or protostellar nature, range of (deconvolved) FWHM sizes and masses.

<sup>(2)</sup> Values modified using  $T_{\text{dust}} = 15$  K instead of  $T_{\text{dust}} = 20 - 25$  K.

efficiency is  $\gtrsim 50 - 70\%$  for each prestellar condensation of  $\rho$  Oph.

Interestingly, the starless H<sup>13</sup>CO<sup>+</sup> condensations detected by Onishi et al. in Taurus also have a mass spectrum that resembles, for  $m > 3.5 M_{\odot}$ , the IMF of field stars (OMFK01, this volume). In marked contrast with CO results (see Fig. 4 and, e.g., Williams et al. 2000), this finding suggests that high density molecular tracers can also give access to the real progenitors of protostars. The star formation efficiency estimated by OMKF01 for their condensations is significantly lower ( $\lesssim 15\%$ ) than that inferred in protoclusters, which may be characteristic of regions forming stars in relative isolation such as Taurus.

On the other hand, the mass distribution found by submm continuum studies which do not carefully select small-scale pre-stellar fragments (see Sect. 2.2) is generally scale-free and tends to follow the same power-law as that observed for CO clumps (e.g. CGJH00 and SK01). Likewise, the mass spectrum obtained by MAN98 when combining the dense cores *and* compact condensations of  $\rho$  Oph together is roughly scale-free with  $N(> m) \propto m^{-0.5}$ .

The introduction of an upper sizescale in the study of cloud structure naturally creates a break in this self-similar scaling. This may explain why JWM00, who filtered dust structures larger than 21 000 AU in diameter in  $\rho$  Oph, found a mass spectrum reminiscent of the Salpeter IMF above a break at  $m \sim 0.9 M_{\odot}$  (when  $T_{\text{dust}}=15$  K). However, the upper sizescale used to select protocluster condensations must be physically motivated (cf. § 2.1) for the derived mass spectrum to be meaningful.

### 3.2. Mass-size relation of protocluster condensations

Figure 5 compares the mass-size relations derived for the (sub)mm dust continuum condensations of the  $\rho$  Oph and NGC 2068/2071 protoclusters (from

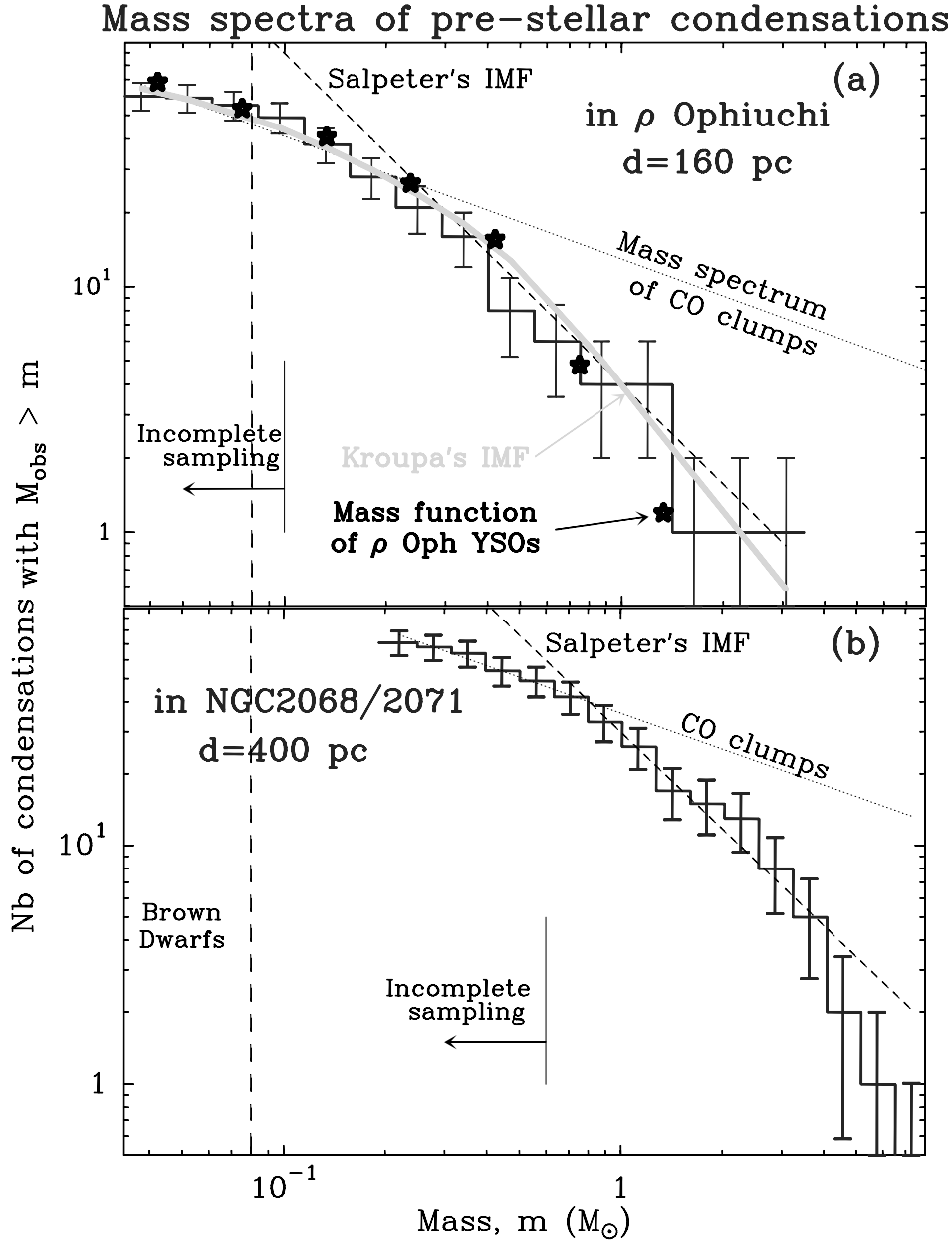


Figure 4. Cumulative mass distributions of the pre-stellar condensations in the  $\rho$  Oph (a) and NGC 2068/2071 (in b) protoclusters (from MAN98 and MAWB01). The dotted and dashed lines show power-laws of the form  $N(> m) \propto m^{-0.5}$  (mass spectra of CO clumps, see Williams et al. 2000) and  $N(> m) \propto m^{-1.35}$  (IMF of Salpeter 1955), respectively. The continuous curve in (a) shows the shape of the field star IMF (Kroupa et al. 1993). The star markers in (a) represent the mass function of  $\rho$  Oph YSOs derived from an extensive mid-IR survey with ISOCAM (Bontemps et al. 2001; Kaas & Bontemps, this volume). The error bars correspond to  $\sqrt{N}$  counting statistics.

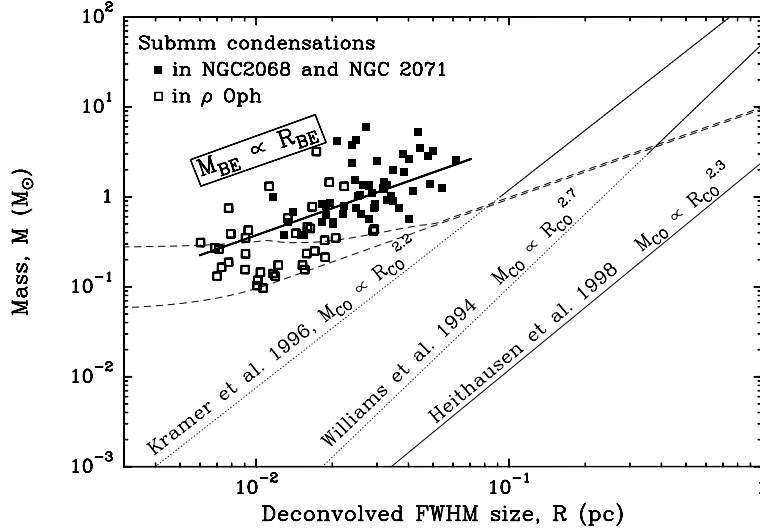


Figure 5. Mass-size relation of the starless submm condensations identified by MAN98 and MAWB01 in the  $\rho$  Oph and NGC 2068/2071 protoclusters (open and filled squares, respectively). The thick solid line is the mass-size relation expected for critical Bonnor-Ebert spheres (see text). The two dashed curves show the  $5\sigma$  detection threshold as a function of size in the two protoclusters.

MAN98 and MAWB01) with those found for CO clumps in various clouds (e.g. Heithausen et al. 1998). The (sub)mm condensations are definitely denser ( $n_{\text{H}_2} \gtrsim 10^6 \text{ cm}^{-3}$ ) than both CO clumps ( $n_{\text{H}_2} \sim 10^3 \text{ cm}^{-3}$ ) and typical  $\text{NH}_3$  cores ( $n_{\text{H}_2} \sim 10^4 - 10^5 \text{ cm}^{-3}$  – Jijina, Myers, & Adams 1999). The mass-size relation of the condensations spans only one decade in size and is much flatter than that of CO clumps: a formal fitting analysis gives  $M_{\text{smm}} \propto R_{\text{smm}}^{1.1}$  as opposed to  $M_{\text{CO}} \propto R_{\text{CO}}^{2.4}$ . Although the observed correlations may be partly affected by size-dependent detection thresholds, it is worth pointing out that they are suggestive of a change from a turbulence-dominated to a gravity-dominated regime. Indeed, while the Larson law  $M \propto R^2$  is consistent with the fractal, turbulent nature of molecular clouds (e.g. Elmegreen & Falgarone 1996), a linear relation ( $M \propto R$ ) is expected for a sample of self-gravitating isothermal condensations assuming a uniform temperature and a range of external pressures (cf. Bonnor 1956). The thick solid line in Fig. 5 displays the  $M(R) = 2.4 R a^2/G$  relation obtained for critical Bonnor-Ebert spheres when  $T = 15 \text{ K}$  ( $a$  is the sound speed). A very similar linear relation ( $M(R) = 2 R a^2/G$ ) holds for truncated singular isothermal spheres (cf. Shu 1977). The largest condensations of NGC 2068/2071 are consistent with  $P_s \sim 10^5 k_B \text{ cm}^{-3} \text{ K}$ , and the smallest condensations of  $\rho$  Oph with  $P_s \sim 10^7 k_B \text{ cm}^{-3} \text{ K}$ . These values are compatible with the range of ambient pressures expected in protoclusters (cf. Myers 1998 and Johnstone et al. 2000). Although the Bonnor-Ebert isothermal model is probably too simplistic to fully describe the condensations observed in protoclusters, the comparison

shown in Fig. 5 is quite encouraging. It illustrates that *the pre-stellar condensations identified in the dust continuum are much more centrally concentrated than CO clumps and require the effects of self-gravity.*

#### 4. Conclusions

There is now a growing body of evidence that the fragmentation of dense ( $\sim 10^5 - 10^6 \text{ cm}^{-3}$ ) cores into compact, self-gravitating condensations determines the IMF of star clusters in the low- to intermediate-mass range ( $0.1 - 5 M_\odot$ ). A plausible scenario, supported by some numerical simulations of cluster formation (Klessen & Burkert 2000; Padoan et al. 2001), could be the following: First, cloud turbulence generates a field of density fluctuations, a fraction of them corresponding to self-gravitating fragments; second, these fragments (or “kernels”) decouple from their turbulent environment (e.g. Myers 1998) and collapse to protostars after little interaction with their surroundings.

More extensive surveys should be done to improve the statistics and search for starless condensations more massive than  $10 M_\odot$ . However, high-mass stars may not form from the collapse of single condensations but from the merging of several pre-/proto-stellar condensations of low to intermediate mass. In the collision scenario of Bonnell, Bate, & Zinnecker (1998), the cluster crossing time must be short enough to allow individual condensations to collide and coalesce with one another. Follow-up high-resolution dynamical studies in dense molecular tracers are thus necessary to decide whether the condensations detected in the submm dust continuum have the potential to form massive stars with  $M_\star \gtrsim 10 M_\odot$ . Preliminary results of such a dynamical study suggest that this is not the case in the  $\rho$  Oph protocluster (Belloche et al., this volume).

Deeper, wider submillimeter continuum surveys in a variety of star-forming regions are clearly required to set stronger constraints on the IMF’s origin and investigate possible environmental effects. At the end of the present decade, the FIRST/Herschel satellite equipped with the bolometer arrays SPIRE and PACS will carry out unbiased surveys of nearby ( $d \lesssim 1 \text{ kpc}$ ) cloud complexes at 90–300  $\mu\text{m}$ , i.e., at wavelengths where cold pre-stellar condensations emit most of their radiation. Thanks to its unprecedented resolution and sensitivity around  $\lambda \sim 0.8\text{--}1 \text{ mm}$  (and below), the ALMA interferometer will make possible similar investigations in distant protoclusters including Galactic mini-starburst regions.

**Acknowledgments.** We acknowledge useful discussions with Anthony Whitworth on the mass-size relation of submm condensations given in Fig. 5.

#### References

- André, P., Ward-Thompson, D., Barsony, M. 2000, in *Protostars & Planets IV*, ed. V. Mannings, A. Boss, & S. Russell (Tucson: Univ. Arizona Press), p. 59
- Bacmann, A., André, P., Puget, J.-L., Abergel, A., Bontemps, S., & Ward-Thompson, D. 2000, *A&A*, 361, 555
- Bertoldi, F., & McKee, C.F. 1992, *ApJ*, 395, 140
- Blitz, L., & Williams, J. P. 1997, *ApJ*, 488, L145

- Bonnell, I. A., Bate, M. R., & Zinnecker, H. 1998, *MNRAS*, 298, 93
- Bonnor, W. B. 1956, *MNRAS*, 116, 351
- Bontemps, S., André, P., Kaas, A., et al. 2001, *A&A*, in press
- Chini, R., Reipurth, B., Ward-Thompson, D., et al. 1997, *ApJ*, 474, L135
- Coppin, K. E. K., Greaves, J. S., Jenness, T., & Holland, W. S. 2000, *A&A*, 356, 1031 (CGJH00)
- Elmegreen, B. G., & Falgarone, E. 1996, *ApJ*, 471, 816
- Evans, N. J., Rawlings, J. M. C., Shirley, Y. L., & Mundy, L. G. 2001, in prep.
- Goodman, A. A., Barranco, J. A., Wilner, D. J., Heyer, M. H. 1998, *ApJ*, 504, 22
- Heithausen, A., Bensch, F., Stutzki, J., Falgarone, E., Panis, J.-F. 1998, *A&A*, 331, L65
- Jijina, J., Myers, P. C., & Adams, F.C. 1999, *ApJS*, 125, 161
- Johnstone, D., Wilson, C. D., Moriarty-Schieven, G., et al. 2000, *ApJ*, 545, 3274 (JWM00)
- Klessen, R. S., & Burkert, A. 2000, *ApJS*, 128, 287
- Kramer, C., Stutzki, J., Winnewisser, G. 1996, *A&A*, 307, 915
- Kramer, C., Stutzki, J., Rohrig, R., & Corneliussen, U. 1998, *A&A*, 329, 249
- Kroupa, P., Tout, C. A., & Gilmore, G. 1993, *MNRAS*, 262, 545
- Lada, E. A., Bally, J., Stark, A. A. 1991a, *ApJ*, 368, 432 (LBS)
- Lis, D. C., Serabyn, E, Keene, J., et al. 1998, *ApJ*, 509, 299
- Loren, R. B., Wootten, A., Wilking, B. A. 1990, *ApJ*, 365, 229
- Masunaga, H., & Inutsuka, S. 2000, *ApJ*, 531, 350
- Motte, F., & André, P. 2001, *A&A*, 365, 440
- Motte, F., André, P., & Neri, R. 1998a, *A&A*, 336, 150 (MAN98)
- Motte, F., André, P. Neri, R., & Abergel, A. 1998b, in *ASP Conf. Ser. Vol. 132, Star Formation with the Infrared Space Observatory*, ed. J. Yun & R. Liseau, 163
- Motte, F., André, P., Ward-Thompson, D., Bontemps, S. 2001, submitted (MAWB01)
- Myers, P. C. 1998, *ApJ*, 469, L109
- Salpeter, E. E. 1955, *ApJ*, 121, 161
- Sandell, G., & Knee, L.B.G. 2001, *ApJ*, 546, L49 (SK01)
- Shu, F. H. 1977, *ApJ*, 214, 488
- Starck, J.-L., Murtagh, F., & Bijaoui, A. 1998, *Image Processing and Data Analysis: The Multiscale Approach*, Cambridge: Cambridge Univ. Press
- Testi, L., Sargent, A. I. 1998, *ApJ*, 508, L91 (TS98)
- Williams, J. P., de Geus, E. J., Blitz, L. 1994, *ApJ*, 428, 693
- Williams, J. P., Blitz, L., McKee, C. F. 2000, in *Protostars & Planets IV*, ed. V. Mannings, A. Boss, & S. Russell (Tucson: Univ. Arizona Press), p. 97